TECHNICAL REPORT

IEC TR 62383

First edition 2006-01

Determination of magnetic loss under magnetic polarization waveforms including higher harmonic components – Measurement, modelling and calculation methods

anodelling as a modelling as a model



Publication numbering

As from 1 January 1997 all IEC publications are issued with a designation in the 60000 series. For example, IEC 34-1 is now referred to as IEC 60034-1.

Consolidated editions

The IEC is now publishing consolidated versions of its publications. For example, edition numbers 1.0, 1.1 and 1.2 refer, respectively, to the base publication, the base publication incorporating amendment 1 and the base publication incorporating amendments 1 and 2.

Further information on IEC publications

The technical content of IEC publications is kept under constant review by the IEC, thus ensuring that the content reflects current technology. Information relating to this publication, including its validity, is available in the IEC Catalogue of publications (see below) in addition to new editions, amendments and corrigenda. Information on the subjects under consideration and work in progress undertaken by the technical committee which has prepared this publication, as well as the list of publications issued, is also available from the following:

IEC Web Site (<u>www.iec.ch</u>)

. Catalogue of IEC publications

The on-line catalogue on the IEC web site (www.iec.ch/searchpub) enables you to search by a variety of criteria including text searches, technical committees and date of publication. On-line information is also available on recently issued publications, withdrawn and replaced publications, as well as corrigenda.

• IEC Just Published

This summary of recently issued publications (www.iec.ch/online_news/ justpub) is also available by email. Please contact the Customer Service Centre (see below) for further information.

• Customer Service Centre

If you have any questions regarding this publication or need further assistance, please contact the Customer Service Centre:

Email: <u>custserv@iec.ch</u>
Tel: +41 22 919 02 11
Fax: +41 22 919 03 00

TECHNICAL REPORT

IEC TR 62383

First edition 2006-01

62303.206 **Determination of magnetic loss** under magnetic polarization waveforms including higher harmonic components ing

ing

cick to view the full poly

cick to view the full poly

ECNORM. Measurement, modelling and calculation

© IEC 2006 — Copyright - all rights reserved

No part of this publication may be reproduced or utilized in any form or by any means, electronic or mechanical, including photocopying and microfilm, without permission in writing from the publisher.

International Electrotechnical Commission, 3, rue de Varembé, PO Box 131, CH-1211 Geneva 20, Switzerland Telephone: +41 22 919 02 11 Telefax: +41 22 919 03 00 E-mail: inmail@iec.ch Web: www.iec.ch



PRICE CODE

V

CONTENTS

FC	REW	ORD	4		
IN ⁻	TROD	UCTION	6		
1	Scor	De	7		
2		native references			
3	Principles of measurement				
J		General			
	3.1				
	3.2	Yokes, windings and test specimen	8		
	3.3	Noveform synthesizer	٥٥		
	3.4	Power amplifier Waveform synthesizer Digitiser Control of secondary voltage Peak reading apparatus Air flux compensation	٥٥		
	3.5	Control of accordance with a control of accor	٥٥		
	3.6	Control of Secondary Voltage	9		
	3.7	A in flow, apparation	9		
4	3.8	Air flux compensation	9		
4	wea	suring systemsurements	10		
5	Mea		10		
	5.1	Generation of the magnetic polarization waveform including higher harmonics	10		
	5.2	Determination of peak value of magnetic polarization			
	5.3	Determination of the magnetic polarization			
	5.4	Determination of magnetic field strength			
	5.5	Determination of the magnetic loss			
	5.6	Plotting the a.c. hysteresis loop including the higher harmonics			
6		mple of measurement			
•	6.1	Magnetic loss measurement of non-oriented electrical steel sheets			
	6.2	Magnetic loss measurement under stator tooth waveform conditions			
7		liction of magnetic loss including higher harmonic polarization			
'	7.1	General			
	7.1 7.2	Energy loss separation [14]			
	7.2	Neural network method [17]			
	7.3 7.4	Modified superposition formula [20]			
8					
		mary -			
Bit	oliogra	phy	31		
		Block diagram of the measuring system for the measurement of magnetic lectrical steel sheets under magnetic polarization waveforms which include			
		armonic components	10		
Fig	jure 2	a – Magnetic polarization $J(t)$	13		
Fig	jure 2	b – Magnetic field strength <i>H(t)</i>	14		
Fig	jure 2	c – AC hysteresis loops	14		
ma	gneti	– Dependency on the higher harmonic polarization components of the components of the polarization $J(t)$; magnetic field strength $H(t)$, and a.c. hysteresis loops of nted electrical steel at a fundamental magnetizing frequency f_1 = 60 Hz and a			
		m magnetic polarization \hat{J} = 1,5 T, and for higher harmonic frequency of			
₹h=	-231 ₁ .		14		

Figure 3 – Specific total loss depending on the higher harmonic frequency and higher	
harmonic polarization for the non-oriented electrical steel sheet at \hat{J} = 1,5 T	15
Figure 4 – <i>B</i> -coil winding positions of stator tooth of a 3,75 kW induction motor to measure the a.c. hysteresis of the stator tooth depending on the load	16
Figure 5 – AC hysteresis loop of the stator teeth of a 3,75 kW induction motor measured in single sheet tester	16
Figure 6 – Specific total loss of the stator tooth depending on the load	17
Figure 7 – Examples of experimental dependence of the quantity $W_{dif} = W - W_{cl} = W_h + W_{exc}$ on the square root of frequency in grain-oriented Fe-Si laminations (thickness 0,29 mm)	19
Figure 8 – Energy loss per cycle <i>W</i> and its analysis in a non-oriented Fe-(3wt %)Si lamination energy loss with arbitrary flux waveform and minor loops	20
Figure 9 – Examples of composite experimental (solid lines) and reconstructed	
(dashed lines) d.c. hysteresis loops at peak magnetization \hat{J} = 1,4 T in non-oriented Fe-(3 wt %) Si laminations (thickness 0,34 mm) generated by the $J(t)$ waveforms	22
Figure 10 – Experimental dependence of the statistical parameter of the magnetization process $V_{ m o}$ on the peak magnetization value in the tested non-oriented Fe-Si laminations	22
Figure 11 – Loss evolution with the number of minor loops in a non-oriented Fe-Si	
lamination, subjected to controlled constant magnetization rate $\left \frac{dJ(t)}{dt} \right = 4 f \cdot (\hat{J} + 2J_m)$,	
with \hat{J} = 1,4 T and $2nJ_m$ = 1,2 T	23
Figure 12 – Artificial neuron (also termed as with or nodes)	23
Figure 13 – Neural network design topology	
Figure 14 – Waveforms of $\dfrac{dJ(t)}{dt}$, $H(t)$ and $J(t)$ when higher harmonic polarization	
is included	26
Figure 15 – Generation of two symmetrical a.c. minor loop measured in zero polarization region, and in saturation polarization region, of the fundamental hysteresis loop; magnetization in the rolling direction and perpendicular to the rolling direction	27
Figure 16 – Specific total loss $P_{\rm C}$ of the combined waves, with harmonic frequency 23 $f_{\rm 1}$, depending on the position of a.c. minor loop at maximum magnetic polarization of 1,0 T and of 1,5 Trespectively	27
Figure 17 – Specific total loss depending on the higher harmonic frequency	
Figure 18 Constant k_2 vs. peak value of magnetic polarization \hat{J}	
Table 1 – Network design	24
Table 2 – Error of the specific total loss recalled from the trained neural network compared with the measured values at 1,6 T (point not used during the training)	25
Table 3 – Error of the specific total loss recalled from the trained neural network compared with the measured values at 1,5 T (point used during the training)	25

INTERNATIONAL ELECTROTECHNICAL COMMISSION

DETERMINATION OF MAGNETIC LOSS UNDER MAGNETIC POLARIZATION WAVEFORMS INCLUDING HIGHER HARMONIC COMPONENTS – MEASUREMENT, MODELLING AND CALCULATION METHODS

FOREWORD

- 1) The International Electrotechnical Commission (IEC) is a worldwide organization for standardization comprising all national electrotechnical committees (IEC National Committees). The object of IEC is to promote international co-operation on all questions concerning standardization in the electrical and electronic fields. To this end and in addition to other activities, IEC publishes International Standards, Technical Specifications, Technical Reports, Publicly Available Specifications (PAS) and Guides (hereafter referred to as "IEC Publication(s)"). Their preparation is entrusted to technical committees; any IEC National Committee interested in the subject dealt with may participate in this preparatory work. International governmental and non-governmental organizations liaising with the IEC also participate in this preparation. IEC collaborates closely with the International Organization for Standardization (ISO) in accordance with conditions determined by agreement between the two organizations.
- 2) The formal decisions or agreements of IEC on technical matters express, as hearly as possible, an international consensus of opinion on the relevant subjects since each technical committee has representation from all interested IEC National Committees.
- 3) IEC Publications have the form of recommendations for international use and are accepted by IEC National Committees in that sense. While all reasonable efforts are made to ensure that the technical content of IEC Publications is accurate, IEC cannot be held responsible for the way in which they are used or for any misinterpretation by any end user.
- 4) In order to promote international uniformity, IEC National Committees undertake to apply IEC Publications transparently to the maximum extent possible in their national and regional publications. Any divergence between any IEC Publication and the corresponding national or regional publication shall be clearly indicated in the latter
- 5) IEC provides no marking procedure to indipate its approval and cannot be rendered responsible for any equipment declared to be in conformity with an IEC Publication.
- 6) All users should ensure that they have the latest edition of this publication.
- 7) No liability shall attach to IEC or its directors, employees, servants or agents including individual experts and members of its technical committees and IEC National Committees for any personal injury, property damage or other damage of any nature whatsoever, whether direct or indirect, or for costs (including legal fees) and expenses arising out of the publication, use of, or reliance upon, this IEC Publication or any other IEC Publications.
- 8) Attention is drawn to the Normative references cited in this publication. Use of the referenced publications is indispensable for the correct application of this publication.
- 9) Attention is drawn to the possibility that some of the elements of this IEC Publication may be the subject of patent rights. IEC shall not be held responsible for identifying any or all such patent rights.

The main task of IEC technical committees is to prepare International Standards. However, a technical committee may propose the publication of a technical report when it has collected data of a different kind from that which is normally published as an International Standard, for example "state of the art".

IEC/TR 62383, which is a technical report, has been prepared by IEC technical committee 68: Magnetic alloys and steels.

The text of this technical report is based on the following documents:

Enquiry draft	Report on voting		
68/309/DTR	68/315/RVC		

Full information on the voting for the approval of this technical report can be found in the report on voting indicated in the above table.

This publication has been drafted in accordance with the ISO/IEC Directives, Part 2.

The committee has decided that the contents of this publication will remain unchanged until the maintenance result date indicated on the IEC web site under "http://webstore.iec.ch" in the data related to the specific publication. At this date, the publication will be

- reconfirmed,
- withdrawn,
- replaced by a revised edition, or
- amended.

A bilingual version of this publication may be issued at a later date.

ECHORN.COM. Click to view the full PDF of IEC TR. 62383: 2006

INTRODUCTION

The specific total loss has to be measured for the design of electrical machines and classification of electrical steel sheets. During the last 20 years, electrical engineers have determined the magnetic induction waveforms of electrical machines [1] to [4]¹⁾, and calculated the magnetic power loss under non-sinusoidal waveform of magnetic polarization [5] to [13]. They designed electrical machines using numeric calculation (FEM, BEM) and high speed computers, including non-linear and hysteresis properties of magnetic materials.

Under standard measurement conditions, the specific total loss of electrical steel is to be measured only under the condition of sinusoidal waveform of the magnetic polarization. However, the actual magnetic polarization waveforms of the electric machine are almost always not sinusoidal because of the material behaviour (anisotropy, non-linear B-H performance in high polarization regions such as the stator tooth of electrical machines), because of PWM modulated voltage for variable speed motors and because of the layout of the magnetic circuit and the winding scheme (tooth harmonics).

Specific total loss values obtained by the standard method are not really applicable to an actual electrical machine design because the specific total loss of ferromagnetic material cannot be predicted easily due to non-linear and hysteresis effects, but these higher harmonic polarizations bring about a large increase in magnetic loss.

¹⁾ The figures in square brackets refer to the Bibliography.

DETERMINATION OF MAGNETIC LOSS UNDER MAGNETIC POLARIZATION WAVEFORMS INCLUDING HIGHER HARMONIC COMPONENTS – MEASUREMENT, MODELLING AND CALCULATION METHODS

1 Scope

Nowadays, by computer aided testing (CAT), a.c. magnetic properties of electrical steel sheets can be measured under various measuring conditions automatically. For example, the magnetic loss in the presence of higher harmonic frequency components of magnetic polarization can be measured using the arbitrary waveform synthesizer, digitiser and computer.

The present standard methods (IEC 60404-2, IEC 60404-3 and IEC 60404-10) for the determination of specific total loss are restricted to the sinusoidal waveform of magnetic polarization, and these standards are still important for the characterization of core materials. However, actual waveforms of magnetic polarization in the electrical machines and transformers always include higher harmonic polarizations, and nowadays electrical machines can be designed using numerical methods including higher harmonics. But for these conditions, there is still no standard testing method.

This technical report reviews methods for measurement of the magnetic loss of soft magnetic materials under the condition of magnetic polarization which includes higher harmonic components.

2 Normative references

The following referenced documents are indispensable for the application of this document. For dated references, only the edition cited applies. For undated references, the latest edition of the referenced document (including any amendments) applies.

IEC 60404-2, Magnetic materials – Part 2: Methods of measurement of the magnetic properties of electrical steel sheet and strip by means of an Epstein frame

IEC 60404-3:1992, Magnetic materials – Part 3: Methods of measurement of the magnetic properties of magnetic sheet and strip by means of a single sheet tester

IEC 60404-6, Magnetic materials – Part 6: Methods of measurement of the magnetic properties of magnetically soft metallic and powder materials at frequencies in the range 20 Hz to 200 kHz by the use of ring specimens

IEC 60404-10, Magnetic materials – Part 8: Specifications for individual materials – Section 10: Specification for magnetic materials (iron and steel) for use in relays

3 Principles of measurement

3.1 General

The described method of measurement with the inclusion of higher harmonics is, in principle, also applicable using the Epstein frame or a ring core as a magnetic circuit. With the Epstein frame, one should be aware of the particular path length characteristics which are also not exactly known in the higher frequency range.

The proposed test apparatus is based on the magnetic circuit of a double U-yoke SST. It can be considered to consist of the following parts.

3.2 Yokes, windings and test specimen

Each yoke is formed in the shape of a U and is made up of an insulated sheet of electrical steel or nickel iron alloy. The construction methods of yokes could follow the instructions of Annex A of IEC 60404-3. The dimensions of the yokes and specimen are not restricted, but if the yoke size becomes smaller, the effective magnetic path length $l_{\rm eff}$ should be equal to the inside width corresponding to the procedure given in IEC 60404-3. It is preferable that the initial permeability of the yoke should be reasonably constant with frequency up to the maximum higher harmonic frequency to be measured. Regarding the windings and the test specimen, it should again be referred to IEC 60404-3 and, in the case of ring specimens, to IEC 60404-6.

Capacitance and dielectric effects become an issue for higher frequency components. The dielectric loss should be minimised by careful management of the winding space and dielectric constants of the formers and wire insulation.

The temperature of the test specimen should be measured at all times. For higher frequency measurements, the temperature rise becomes a major factor and steps should be taken to minimize this.

3.3 Power amplifier

The power amplifier shall have low output impedance, and the frequency bandwidth of the power amplifier should be higher than the highest harmonic frequency to be measured. The output voltage of the power amplifier should be high enough to magnetize the specimen over the full higher harmonic frequency range. For details, reference should be made to IEC 60404-2, IEC 60404-3 and IEC 60404-6.

3.4 Waveform synthesizer

An arbitrary waveform can be synthesized by computer programming. The frequency of the generated wave should be synchronized with the digitiser frequency, and the frequency uncertainty of the waveform synthesizer shall be better than 0,01%. The waveform synthesizer output should allow arbitrary waveforms generated by synthesized digital wave data. The relative uncertainty of the frequency should be less than 0,01%.

3.5 Digitiser

For the digitisation of the secondary induced voltage $U_2(t)$ and the voltage $U_s(t)$ across the non-inductive precision resistor R_s which is connected in series with the primary winding to determine the magnetizing current, a 2-channel digitiser is necessary. The 2 channels must be sampled simultaneously and then digitised. Following this, the data are recorded in a memory.

If the length of the period divided by the time interval between the measuring points, i.e. the sampling frequency ratio $f_{\rm S}$ divided by the magnetizing frequency $f_{\rm m}$, is an integer (Nyquist condition), the power integral can be, without mathematical error, be replaced by the corresponding sum. The sum correctly represents the power integral up to the nth harmonic where 2n is the number of samples per fundamental period. Keeping the Nyquist condition is possible only where the sampling frequency $f_{\rm S}$ and the magnetizing frequency $f_{\rm m}$ are synchronized to a common fundamental clock and thus have a fixed integer ratio.

In that case, the hysteresis loop must be scanned using a sampling frequency f_s higher than twice the bandwidth of the B- and H-signals,

$$f_s = 2nf_m \tag{1}$$

where n is the highest harmonic to be measured.

However, the commercial hardware components are not usually synchronized in this way and the ratio $f_{\rm s}/f_{\rm m}$ is then not an integer. In that case, the sampling frequency must be considerably higher (for instance 1 024 samples per period) in order to keep the deviation of the true period length from the closest multiple of intervals of sampled measurements small.

Keeping the Nyquist condition becomes a deciding advantage in the case of higher frequencies. The use of a low-pass antialiasing filter must be considered in order to avoid contributions from low-frequency apparent harmonics which do not exist in the measurement signal. The antialiasing filter must limit the system bandwidth to $\langle f_s/2 \rangle$.

Regarding the amplitude resolution, with a lower than 12-bit resolution, the digitalization error can be considerable, particularly for non-oriented material with high silicon content. Thus, at least a 12-bit amplitude resolution is recommended. Moreover, the two voltage channels should transfer the signals without a significant phase shift. The phase shift should be so small that the total uncertainty is not significantly affected.

When magnetic loss is measured under conditions of magnetic polarization which include higher harmonic components and the higher harmonic amplitude becomes high enough to produce minor loops, the digital sampling condition for the higher harmonics should also satisfy the above described sampling conditions.

3.6 Control of secondary voltage

The waveform of the secondary voltage should be controlled to have the required components. This control can be achieved by feedback techniques using digital or analog means.

The deviation should be below 1 % for each harmonic component.

3.7 Peak reading apparatus

For the measurement of the peak value of the magnetic polarization, a Miller type analog integrator and a peak reader should be used with a frequency bandwidth higher than the highest harmonic frequency f_h to be measured.

The peak reader should be able to repeat peak readings at an appropriate time rate.

The uncertainty of the peak reading apparatus should be better than 0,2 %.

NOTE An average type voltmeter may not be used for measurement of the peak value of the magnetic polarization because the secondary induced voltage may have more than two zero crossing per period.

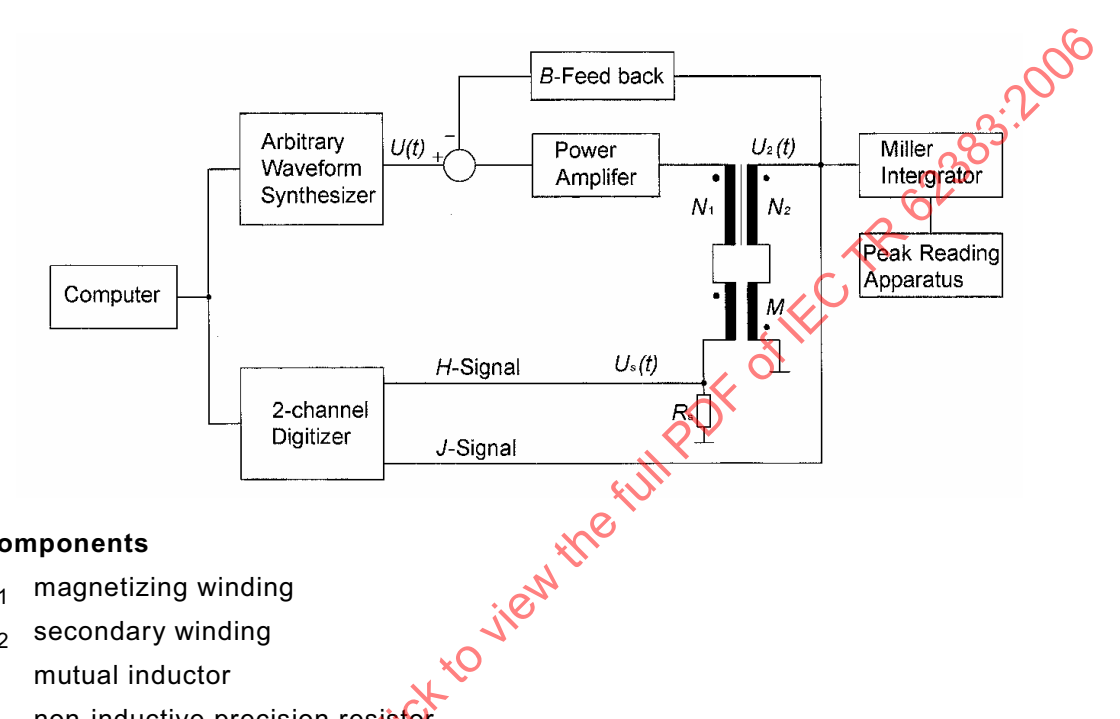
3.8 Air flux compensation

Air flux should be compensated. This can be achieved by a mutual inductor. The primary winding of the mutual inductor is connected in series with the primary winding of the test apparatus, while the secondary winding of the mutual inductor is connected to the secondary winding of the test apparatus in series opposition.

The adjustment of the value of the mutual inductance shall be made so that, when passing an alternating current through the primary windings in the absence of the specimen in the apparatus, the voltage measured between the non-common terminals of the secondary windings shall be no more than 0,1 % of the voltage appearing across the secondary winding of the test apparatus alone.

4 Measuring system

The measuring system can be constructed using the components which are described in Clause 2. The block diagram of the circuit is shown in Figure 1.



Components

N₁ magnetizing winding

 N_2 secondary winding

Μ mutual inductor

R_s non-inductive precision resistor

Figure 1 - Block diagram of the measuring system for the measurement of magnetic loss of electrical steel sheets under magnetic polarization waveforms which include higher harmonic components

5 Measurements

5.1 Generation of the magnetic polarization waveform including higher harmonics

The time dependent magnetic polarization including higher harmonics can be described by

$$J(t) = \sum_{j=0}^{N} J_{(2j+1)} \sin[(2j+1)\omega_1 t + \phi_{(2j+1)}]$$
 (2)

where

is a non-negative integer;

Ν corresponds to the highest harmonic frequency f_h ;

is the fundamental angular frequency($\omega_1 = 2\pi f_1$); ω_1

is the amplitude of the $(2j+1)^{th}$ harmonic at the angular frequency $\omega_h = (2j+1)\omega_1$; $J_{(2j+1)}$

is the phase angle. $\phi_{(2j+1)}$

The synthesized reference voltage U(t) is as follows;

$$U(t) = N_2 A \sum_{j=0}^{N} (2j+1)\omega_1 J_{(2j+1)} \cos[(2j+1)\omega_1 t + \phi_{(2j+1)}]$$
(3)

where

 N_2 is the number of turns of secondary winding;

A is the cross sectional area of specimen.

The procedure of setting the desired magnetic polarization follows the following steps.

First the relative amplitudes of fundamental and higher harmonics waves are set, the resulting peak value of the magnetic polarization is measured and then the gain of the synthesizer is set so that the required amplitude of magnetic polarization is achieved.

5.2 Determination of peak value of magnetic polarization

The peak value of magnetic polarization \hat{J} should be measured using a Miller type analogue integrator and a peak reader. The relation between the peak value of magnetic polarization and the output voltage \hat{U}_I of the peak reader is:

$$\hat{U}_{J} = \frac{N_2 A}{RC} \hat{J}$$
(4)

where RC is the time constant of the Miller integrator.

5.3 Determination of the magnetic polarization

The instantaneous value of the magnetic polarization J(i) at the time t = i/nf of the specimen can be calculated from the secondary induced voltage $U_2(t)$ using the following numeric equation:

$$J(i) = -\frac{1}{N_2 A_s nf} \sum_{k=1}^{i} [U_2(k) + U_2(k+1)]/2 - J_0$$
 (5)

where

i is an integer:

n is the number of sampling points per period;

f is the magnetizing frequency;

 J_0 is the integration constant such that

$$\sum_{i=1}^{n} J(i) = 0$$
(6)

The peak value of the magnetic polarization J(t) is identical to the maximum value of J(i).

5.4 Determination of magnetic field strength

The instantaneous value of the magnetic field strength H(i) at the time t = i/nf can be calculated from the digitised value of the voltage $U_s(i)$ across the non-inductive precision resistor R_s :

$$H(i) = \frac{N_1}{l_{eff} R_s} U_s(i) \tag{7}$$

where

 $l_{\it eff}$ is the effective magnetic path length;

 N_1 is the number of turns of primary winding.

5.5 Determination of the magnetic loss

The magnetic loss $P_{\rm c}$ could be calculated using the data from the 2-channel digitiser, the secondary induced voltage $U_2(t)$ and the voltage $U_s(t)$ across the non-inductive precision resistor R_s which is connected in series with the primary winding:

$$P_c = -\frac{N_1}{n\rho_m N_2 A l_{eff} R_s} \sum_{i=1}^n b_2(i) \cdot U_s(i)$$
(8)

where

 P_c is the specific total loss, in watt per kilogram;

i is an integer;

n is the number of sampling points per period;

 N_1 is the number of turns of primary winding;

 $N_{\mathbf{2}}$ is the number of turns of secondary winding;

A is the cross sectional area of specimen;

 ρ_m is density of the test specimen in kilogram per cubic meter.

5.6 Plotting the a.c. hysteresis loop including the higher harmonics

The a.c. hysteresis loop can be plotted using the magnetic polarization from equation (5) and the magnetic field strength from equation (7).

6 Example of measurement

6.1 Magnetic loss measurement of non-oriented electrical steel sheets

Figure 2 shows the results measured on a specimen of non-oriented electrical steel at the fundamental frequency of 60 Hz and maximum magnetic polarization of \hat{J} of 1,5 T under different harmonic amplitude conditions, Figure 2a shows the magnetic polarization curves, Figure 2b the magnetic field strength curves, and Figure 2c the a.c. hysteresis loops. The higher harmonic frequency is $f_{\rm h} = 23f_{\rm 1}$ and the higher harmonic amplitudes $\hat{J}_{\rm 23}$ amount to 2 %, 5 % and 10 % of $\hat{J}_{\rm 1}$.

Figure 3 shows the total loss depending on the higher harmonic frequency $f_{\rm h}$ and higher harmonic polarization \hat{J}_h for the non-oriented electrical steel sheet at $\hat{J}=1.5$ T. For the case of a 0,5 mm thickness specimen, the total loss depending on the higher harmonic frequency $f_{\rm h}$ and higher harmonic polarization \hat{J}_h was much higher than that of the material with a thickness of 0,35 mm due to the eddy current effect.

6.2 Magnetic loss measurement under stator tooth waveform conditions

For the determination of the a.c. hysteresis loop of the stator-tooth of an induction motor, the magnetic polarization of the tooth can be measured using search coil windings, but the magnetic field strength measurement is not so easy inside the actual motor. One measuring method for the a.c. hysteresis loop of the stator-tooth could be to obtain the amplified induced voltage from the *B*-coil and to connect it directly to the input of the measuring system which is described in Clause 4, and then to measure the a.c. magnetic properties of a specimen consisting of the same material as that of the stator-tooth. In doing so, the gain of the amplifier is adjusted to satisfy equation (9) so that the magnetic polarization of the sample in the yoke meets the same magnetic polarization condition as the stator tooth to be achieved.

$$U_s = (\frac{A_s N_s}{A_m N_m}) U_m \tag{9}$$

where $A_{\rm s}$, $N_{\rm s}$ and $U_{\rm s}$ are the cross sectional areas of the sample, number of *B*-coil windings, and the voltage applied to the single sheet tester, respectively. $A_{\rm m}$, $N_{\rm m}$ and $U_{\rm m}$ are the cross sectional area of the stator tooth, number of *B*-coil windings, and the voltage induced from the *B*-coil of the induction motor, respectively.

For the measurement of the a.c. hysteresis loop of the stator-tooth of an induction motor, we prepared a 10 cm \times 10 cm double U-yoke SST and a 3-phase 3,75 kW induction motor which has 4 poles, 36 stator teeth, and 44 rotor teeth. Two *B*-coils, one in the rolling direction and the other one perpendicular to the rolling direction of the stator core were each wound with 10 turns on only one sheet as shown in Figure 4. In this case, we can not measure magnetic polarization *J* but magnetic induction *B*. When magnetic field strength is not so high, air flux is small compared to the magnetic flux density of the core, we can measure magnetic polarization *J* using the voltage induced from the *B*-coil as an approximation. An a.c. dynamometer may be used to load the induction motor.

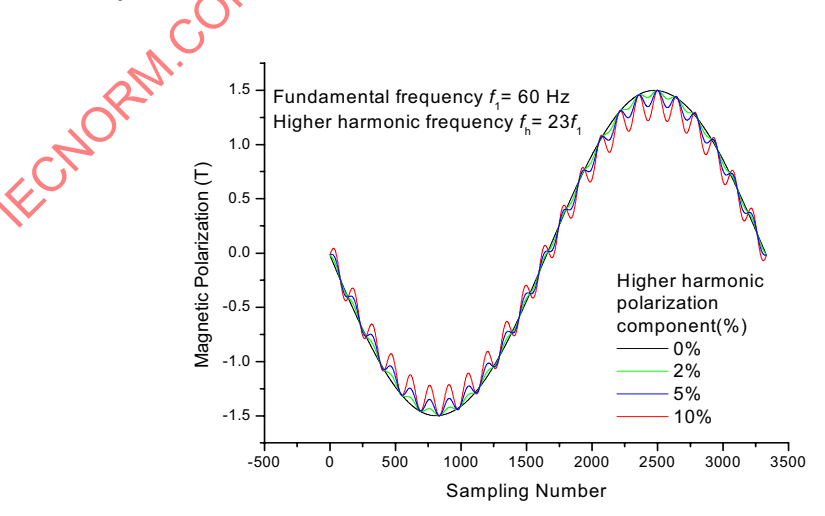


Figure 2a – Magnetic polarization J(t)

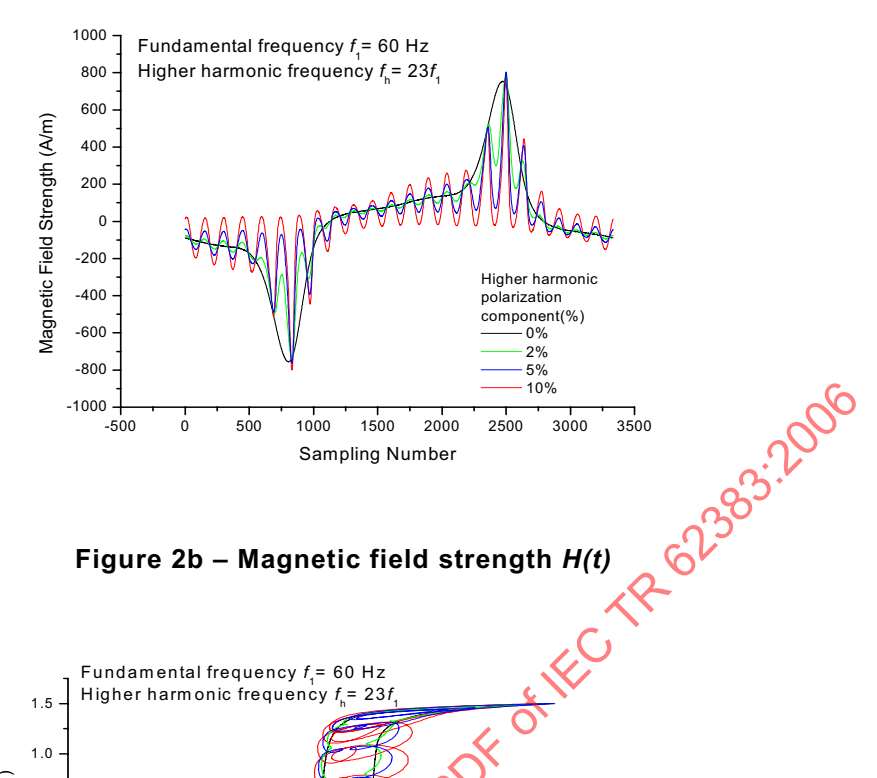


Figure 2b – Magnetic field strength H(t)

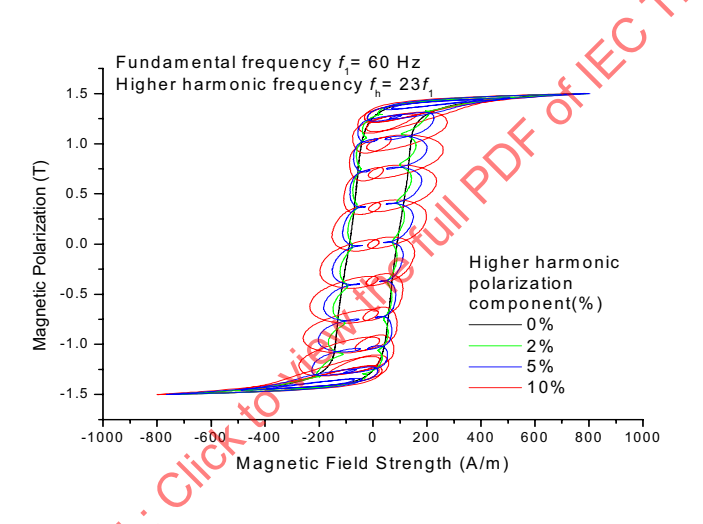


Figure 2c - AC hysteresis loops

The higher harmonic amplitude was 0 %, 2 %, 5 %, and 10 % of \hat{J}_1 respectively.

Figure 2 - Dependency on the higher harmonic polarization components of the magnetic polarization J(t); magnetic field strength H(t), and a.c. hysteresis loops of non-oriented electrical steel at a fundamental magnetizing frequency f_1 = 60 Hz and a maximum magnetic polarization \hat{J} = 1,5 T, and for higher harmonic frequency of f_h =23 f_1

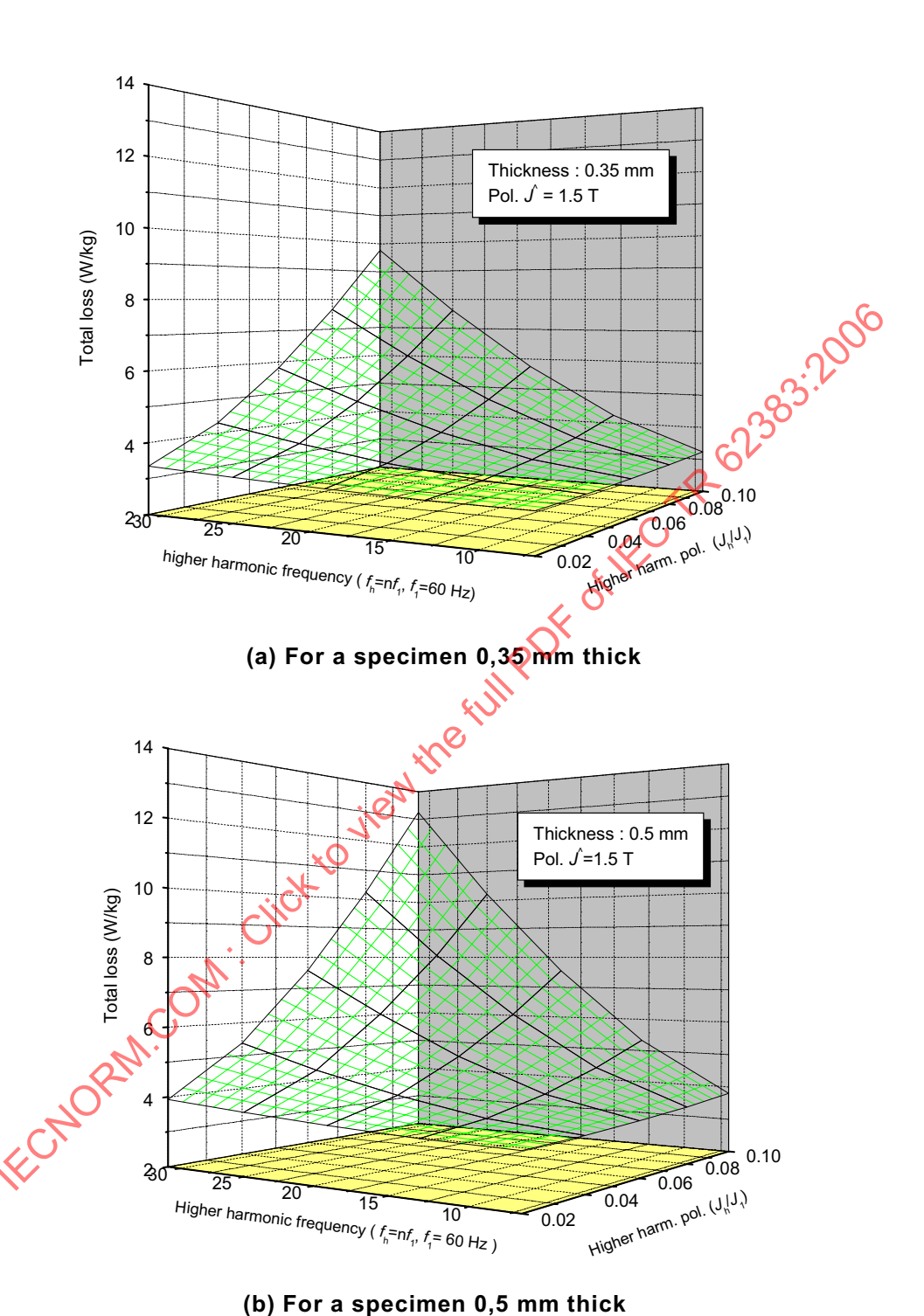


Figure 3 – Specific total loss depending on the higher harmonic frequency and higher harmonic polarization for the non-oriented electrical steel sheet at \hat{J} = 1,5 T

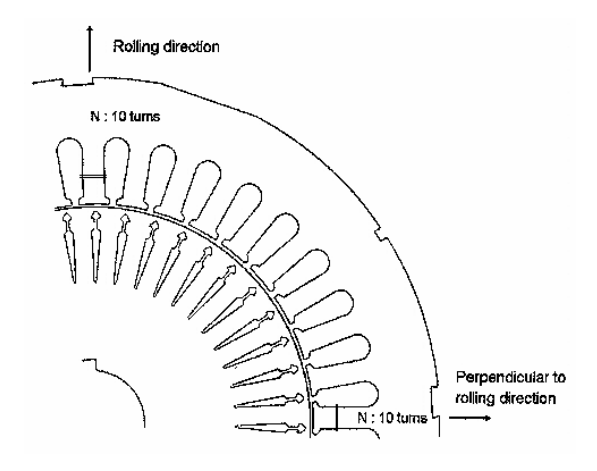


Figure 4 – B-coil winding positions of stator tooth of a 3,75 kW induction motor to measure the a.c. hysteresis of the stator tooth depending on the load

Figure 5 shows the a.c. hysteresis loops for the case of a rotor having no skew, and the B-coil being wound coaxially with the rolling direction of non-oriented electrical steel. Figure 5a shows the a.c. hysteresis loop under sinusoidal magnetic polarization. Figure 5b shows the a.c. hysteresis loop of the stator-tooth under no load, both under the same maximum magnetic polarization \hat{J} however the difference in the specific total loss between the cases of Figure 5a and Figure 5b was more than 10 %. Figure 5e and Figure 5d show a.c. hysteresis loops of the stator-tooth under 40 % and 80 % of the full load. The specific total loss values were increased by more than 30 % and 50 %, respectively. Figure 6 shows the specific total loss depending on the load of the induction motor. The specific total loss also turned out to depend on the direction of magnetization due to the macroscopic magnetic anisotropy of the non-oriented electrical steel.

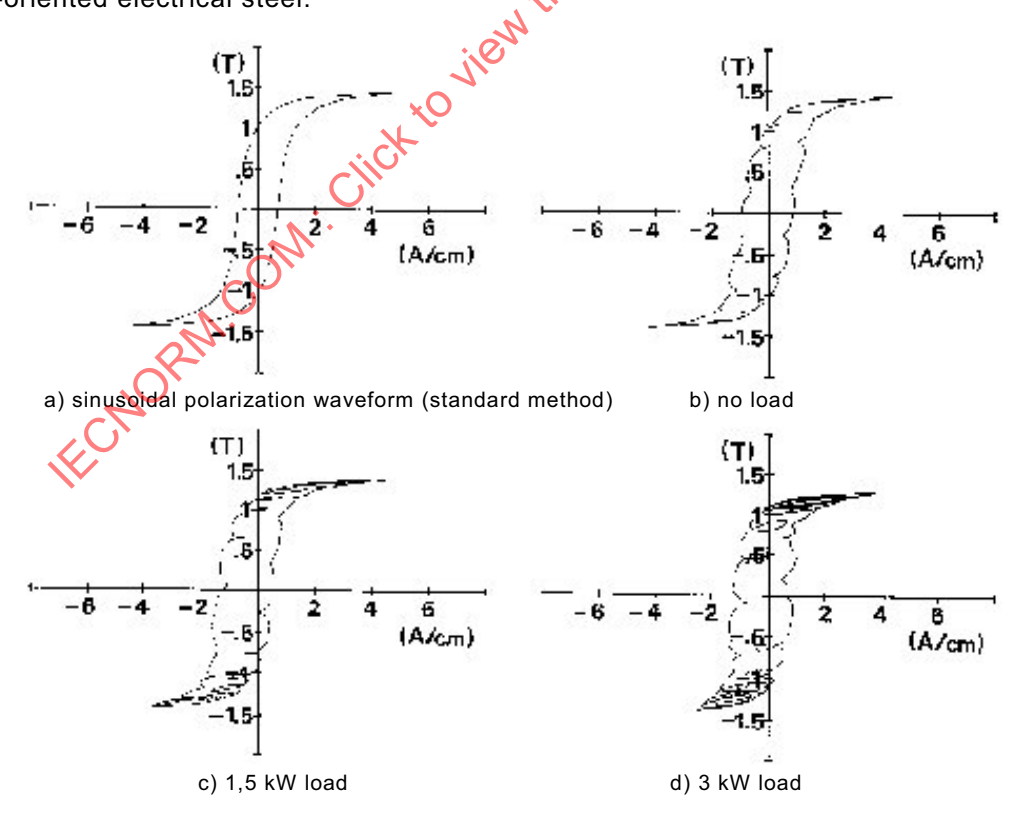
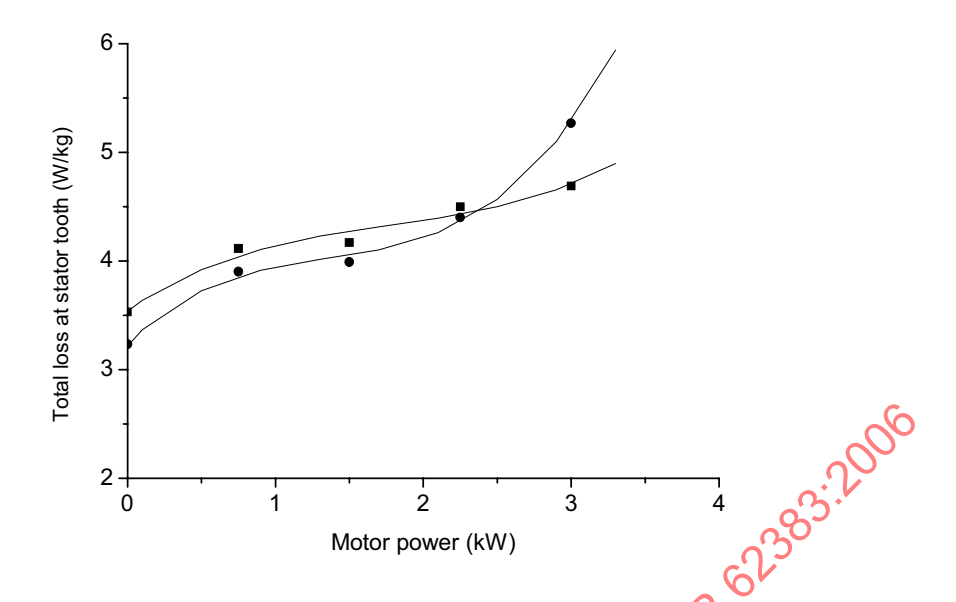


Figure 5 – AC hysteresis loop of the stator teeth of a 3,75 kW induction motor measured in single sheet tester



- : parallel to the rolling direction of non-oriented electrical steel when rotor has no skew
- : perpendicular to the rolling direction of non-oriented electrical steel when rotor has no skew

Figure 6 - Specific total loss of the stator tooth depending on the load

7 Prediction of magnetic loss including higher harmonic polarization

7.1 General

Magnetization process of magnetic materials always shows non-linear and hysteresis behaviour which is very difficult to describe physically. Until now, a hysteresis loop can not be described as a mathematically analytical function. A reasonable model to predict magnetic loss during the magnetization process should be used. Some typical methods which describe the prediction of total loss will be introduced in this report.

7.2 Energy loss separation [14]

7.2.1 General

The physically based separation of specific total loss P(f) at a given frequency f is expressed as the sum of the hysteresis loss P_h , classical eddy current loss $P_{cl}(f)$, and excess loss $P_{exc}(f)$ components

$$P(f) = P_b(f) + P_{cl}(f) + P_{exc}(f)$$
(10)

where $P_h(f) = W_h f$, with W_h the hysteresis energy loss per cycle. Except in a few special cases [15], W_h is always considered as a frequency independent quantity. Equation (10) can then equivalently be written in terms of the energy loss per cycle W = P/f

$$W(f) = W_h + W_{cl}(f) + W_{exc}(f)$$
(11)

There are no limitations, in principle, as to the kind of polarization waveform. The fundamental aim is the prediction of W_h , $W_{cl}(f)$, and $W_{exc}(f)$.

7.2.2 Energy losses with arbitrary flux waveform and no minor loops

The instantaneous classical eddy current loss per unit volume $P_{cl}(t)$ can be defined for a magnetic lamination of conductivity σ and thickness d as

$$P_{cl}(t) = \frac{\sigma d^2}{12} (\frac{dJ(t)}{dt})^2$$
 (12)

This relationship is only valid when the flux penetrates the material completely.

The classical energy loss per cycle T = 1/f is then obtained as

$$W_{cl}(f) = \int_{0}^{T} P_{cl}(t) dt = \int_{0}^{T} \frac{\sigma d^{2}}{12} \left(\frac{dJ(t)}{dt}\right)^{2} dt$$
 (13)

and it can be calculated exactly for all waveforms of J(t).

In the absence of minor loops, the hysteresis loss is independent of the polarization waveform. The instantaneous excess loss $P_{\rm exc}(t)$ is given in its most general form, by equation (14):

$$P_{\text{exc}}(t) = \frac{n_0 V_0}{2} \cdot \left(\sqrt{1 + \frac{4\sigma GSV_0}{n_0^2 V_0^2}} \frac{dJ(t)}{dt} \right) - 1 \cdot \left| \frac{dJ(t)}{dt} \right|$$
 (14)

where

 n_0 is the number of simultaneously active magnetic objects in the limit $f \rightarrow 0$;

 V_0 is a parameter defining the statistics of the magnetic objects;

S is the cross-sectional area of the lamination.

The magnetic object (MO) is defined as an ensemble of neighbouring walls interacting so strongly that they can be treated as a single object. The dynamic behaviour of a single MO is characterized by a damping coefficient G, which is to a good approximation independent of the internal details of the MO. G is a dimensionless parameter and its theoretically calculated value is G=0.135 6. It is stressed that $V_{\rm O}$, which lumps the effect on the excess loss of the material structure, is a function of \hat{J} . In a large number of cases, the value of $n_{\rm O}$ is sufficiently small to ensure that, in all practical respects,

$$\frac{4\sigma GSV_{o}}{n_{o}^{2}V_{o}^{2}} \left| \frac{dJ(t)}{dt} \right| >> 1 \tag{15}$$

and the excess energy loss becomes

$$W_{exc}(f) = \int_0^T P_{exc}(t) dt = \sqrt{\sigma GSV_0} \cdot \int_0^T \left| \frac{dJ(t)}{dt} \right|^{3/2} dt$$
 (16)

which is easily specialized to the desired J(t) waveform.

By combination of equation (11), equation (13) and equation (16), energy loss per cycle becomes as follows:

$$W(f) = W_h + W_{cl}(f) + W_{exc}(f) = W_h + \frac{\sigma d^2}{12} \int_0^T \left(\frac{dJ(t)}{dt}\right)^2 dt + \sqrt{\sigma GSV_o} \cdot \int_0^T \left|\frac{dJ(t)}{dt}\right|^{3/2} dt$$
 (17)

In order to predict the total loss for a given J(t), the following quantities are required: conductivity σ , cross-sectional area S and the pre-emptive determination of W_h and V_0 only. Let us consider the typical experiment in a grain-oriented Fe-Si lamination reported in Figure 7, where the behaviour of the quantity

$$W_{dif}(f) = W(f) - W_{cl}(f) = W_h + W_{exc}(f)$$
(18)

measured under sinusoidal flux, from its best straight fitting line, as provided by equation (18), as a function of $f^{1/2}$. It can be seen that W_h and V_o are obtained from the intercept value and the slope of the theoretical line, respectively.

Figure 8 shows the frequency behaviour of the magnetic energy loss experimentally found in non-oriented Fe-(3 wt %)Si lamination under sinusoidal polarization at peak magnetization $\hat{J}=1,4$ T. The fitting lines have been predicted according to the method outlined in the previous clause, focused on the loss separation equation (18) the direct calculation of W_{cl} and the representation $W_{dif}=W-W_{cl}=W_h+W_{exc}$ as a function of $f^{1/2}$. By this representation the previously contemplated case is met, where W_{dif} exhibits a deviation from the $f^{1/2}$ dependence at low frequencies. Then the best fit of W_{dif} can be made in Figure 8 and provide for the parameters W_{h1} and V_{o} .

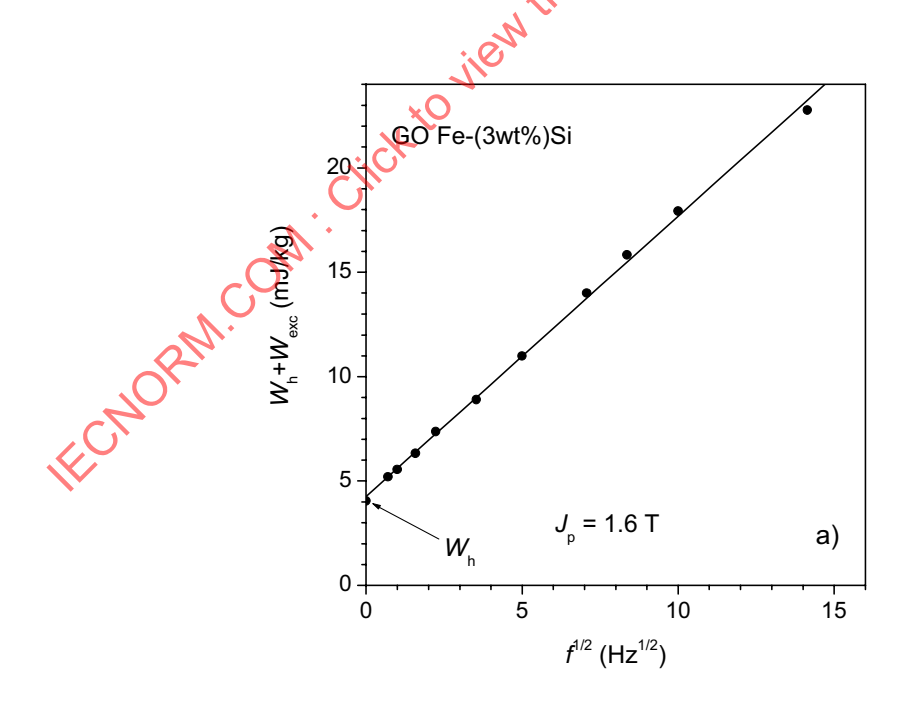
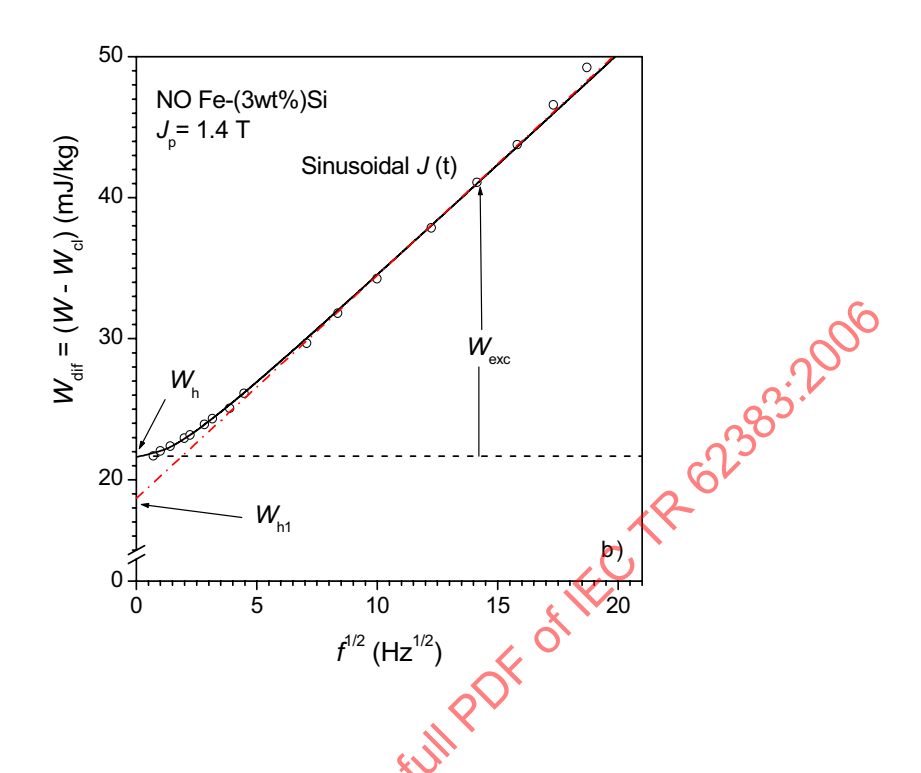


Figure 7 – Examples of experimental dependence of the quantity $W_{dif} = W - W_{cl} = W_h + W_{exc}$ on the square root of frequency in grain-oriented Fe-Si laminations (thickness 0,29 mm)



The experimental quantity $W_{dif} = W - W_{cl} = W_{h} - W_{exc}$ is plotted as a function of $f^{1/2}$. This results in the dash-dot straight fitting line by which the two parameters W_{h1} and V_{o} are determined.

Figure 8 – Energy loss per cycle W and its analysis in a non-oriented Fe-(3wt %)Si lamination energy loss with arbitrary flux waveform and minor loops

For the total loss at a given frequency f in the presence of minor loops, equation (17) should be modified as follows:

$$W = W_{h,M} + W_{h,m} + W_{exc,M} + W_{exc,m} + \frac{\sigma d^2}{12} \int_0^T \left(\frac{dJ(t)}{dt}\right)^2 dt$$
 (19)

where the subscripts M and m apply to major and minor loops, respectively. The quasi-static loss contribution term $W_{h,M} + W_{h,m}$ is then given by the sum of the quasi-static major loop area

 $W_{h,M}$ and the area $W_{h,m} = \sum_{i=1}^{2n} W_{h,m,i}$ resulting from summation of the areas $W_{h,m,i}$ of the 2n minor

loops. These are supposed to be endowed with a polarization swing $\pm J_{m,i}$. $W_{exc,M}$ is the excess energy loss associated with the major loop and $W_{exc,m}$ is the excess energy loss associated with the ensemble of 2n minor loops.

For the calculation of $W_{h,M}+W_{exc,M}$, only the total loss value W_M under sinusoidal polarization at two different frequencies and peak amplitude \hat{J} needs to be known.

$$W_M - W_{cl,M} = W_{h,M} + W_{exc,M} = W_{h1,M} + \sqrt{\sigma GSV_0(J_p)} \cdot \int_{\sum T_M} \left| \frac{dJ(t)}{dt} \right|^{3/2} dt$$
 (20)

under the prescribed waveform J(t) at the desired frequency f. In this equation, the simplification on the analysis of the loss vs. frequency behaviour illustrated in Figure 8 is exploited. $W_{hl,M}$ therefore stands for the linearly extrapolated major loop hysteresis loss term.

It is noticed that the time integration of $|\frac{dJ(t)}{dt}|^{3/2}$ is extended only over the portion $\sum T_M$ of the period T which is not occupied by the minor loops.

To determine $W_{\scriptscriptstyle h,m}$, the simplified Preisach model [14] was used and excess energy loss associated with the ensemble of minor loops

$$W_{exc,m} = \sum_{i=1}^{2n} W_{exc,m,i}$$
 (21)

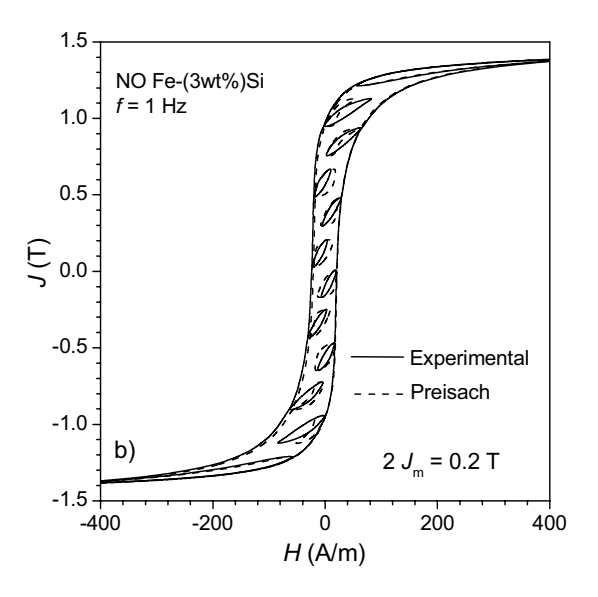
was calculated using the following equation:

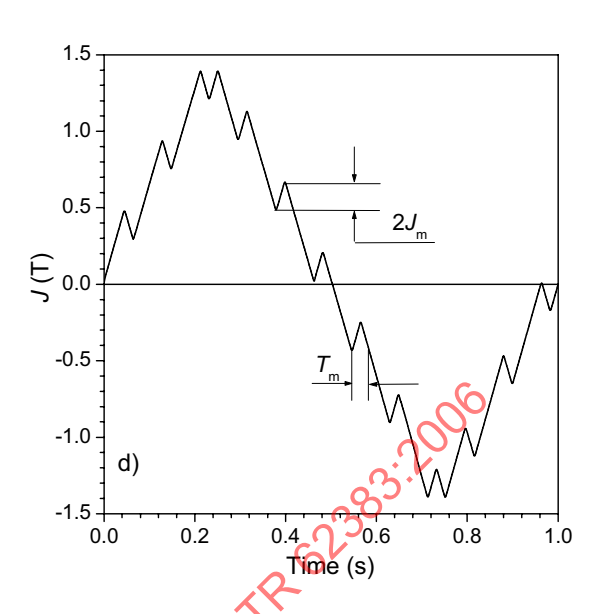
$$W_{exc,m,i} = \sqrt{\sigma GSV_{o}(J_{m,i})} \cdot \int_{T_{m,i}} \left| \frac{dJ(t)}{dt} \right|^{3/2} dt$$
 (22)

where the integration is made over the associated i time interval of duration $T_{m,i}$.

As an example, equation (19) is applied to the prediction of the energy loss in the specific case illustrated in Figure 9, according to the following conditions: \hat{J} = 1,4 T, all minor loops of same peak-to-peak amplitude $2J_m$ and variable number 2n = 2, 4, ...12, with constant value of the product $2n \cdot \Delta J_m$ = 1,2 T.

It may be seen that the parameter $V_0(\hat{J})$, related to the statistical properties of the magnetization process, in particular to the distribution of the local coercive fields, is an increasing function of \hat{J} as illustrated for the present non-oriented Fe-Si lamination in Figure 10. By introducing the results provided by equation (19), we arrive at the prediction shown in Figure 11, which compares well with the experimental data.





The minor loops have peak-to-peak amplitude $2J_m$. The theoretical loops have been reconstructed by means of a Preisach model, using the experimental major hysteresis loop as the sole input information and making suitable simplifying assumptions.

Figure 9 – Examples of composite experimental (solid lines) and reconstructed (dashed lines) d.c. hysteresis loops at peak magnetization \hat{J} = 1,4 T in non-oriented Fe-(3 wt %) Si laminations (thickness 0.34 mm) generated by the J(t) waveforms

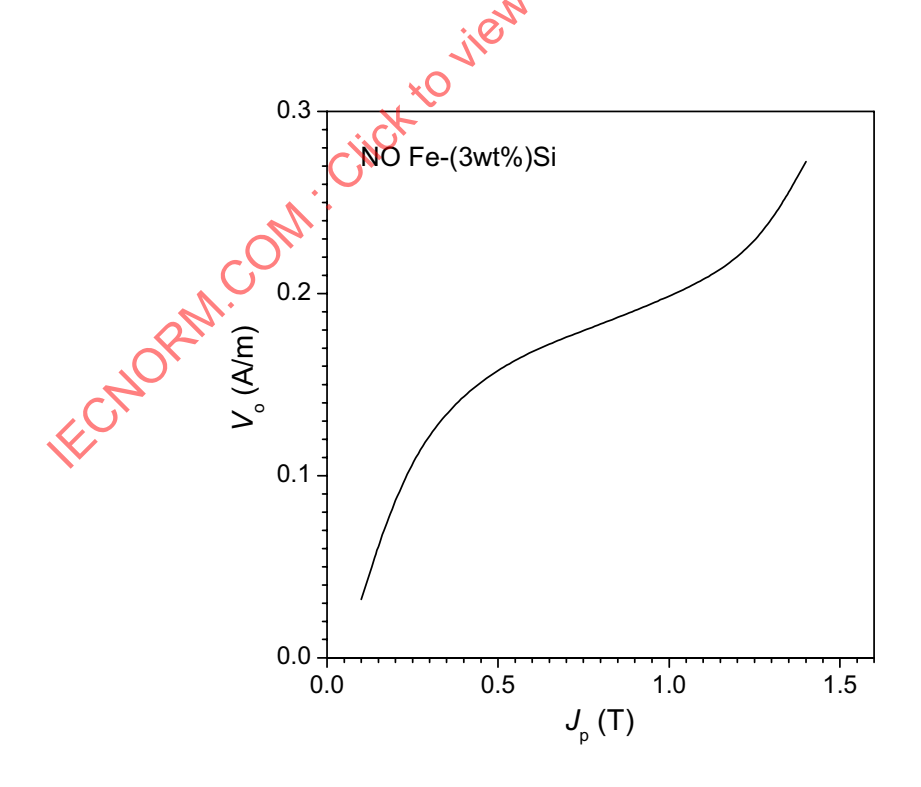


Figure 10 – Experimental dependence of the statistical parameter of the magnetization process $V_{\rm O}$ on the peak magnetization value in the tested non-oriented Fe-Si laminations

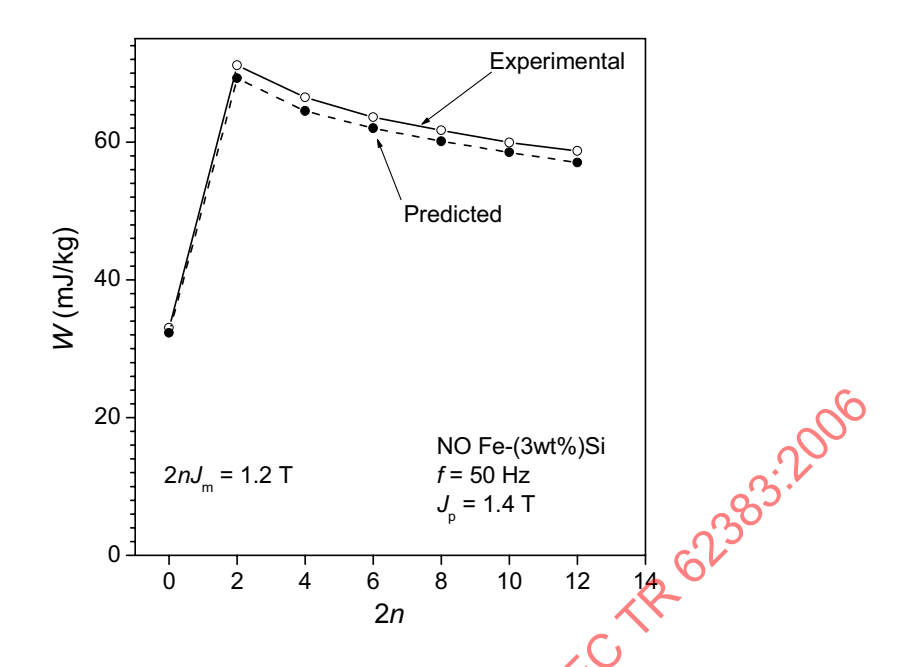


Figure 11 – Loss evolution with the number of minor loops in a non-oriented Fe-Si lamination, subjected to controlled constant magnetization rate $\left| \frac{dJ(t)}{dt} \right| = 4f \cdot (\hat{J} + 2J_m)$

with
$$\hat{J} = 1.4 \text{ T}$$
 and $2nJ_m = 1.2 \text{ T}$

7.3 Neural network method [17]

A neural network is an interconnected assembly of simple processing elements, *units* or *nodes*, shown in Figure 12, whose functionality is loosely based on the animal neuron. The processing ability of the network is stored in the inter-unit connection strengths, or *weights*, obtained by a process of adaptation to, or *learning* from, a set of training patterns [18].

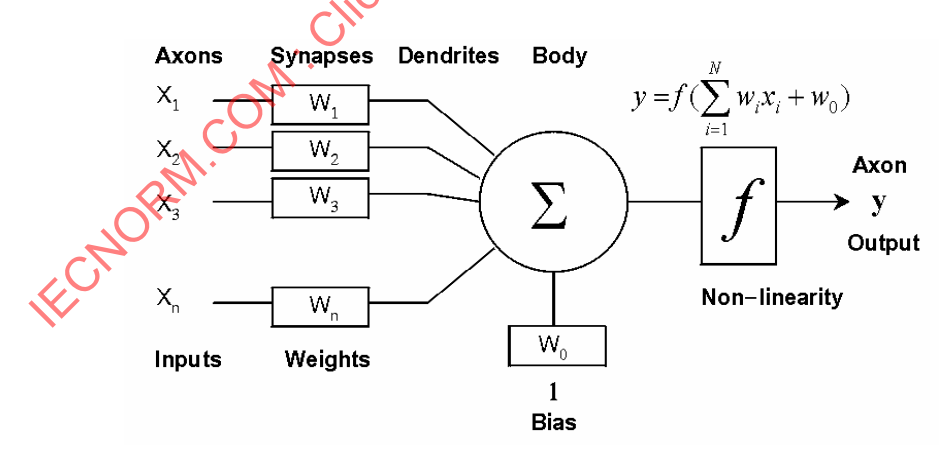


Figure 12 – Artificial neuron (also termed as unit or nodes)

These nodes are organised into groups termed layers, which are distinctly divided into the input layer, hidden layer(s) and output layer, as shown in Figure 13. A network consists of one input layer, one or more hidden layers and one output layer. Connections exist between the nodes of adjacent layers to relay the output signals from one layer to the next. Fully connected networks occur when all nodes in each layer receive connections from all nodes in each preceding layer. Information enters a network through the nodes of the input layer and is distributed to the next processing layer.

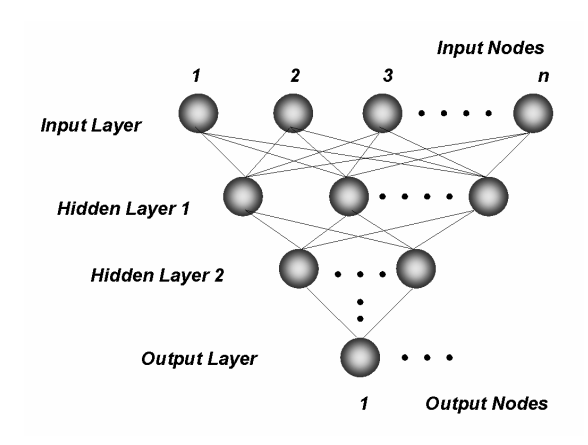


Figure 13 - Neural network design topology

The prediction of loss using a neural network was calculated using the commercial neural network package [19]. It was the aim to predict loss in 0,5 mm thick non-oriented electrical steel with silicon content ranging from 0,2 % to 4 % under sinusoidal, square and PWM waveform excitation at 50 Hz fundamental frequency. Input data was obtained over the flux density range 0,1 T to 1,5 T, the PWM conditions were 50 Hz fundamental frequency, frequency ratio 12 and modulation index varying from 0,5 to 1,0.

In total, four input nodes were used, as shown in Table 1, the peak flux density varying from 0,1 to 1,5 T, the material density varying from 7,85 to 7,60 (10³ kg/m³), the silicon content varying from 0,2 % to 4 % and form factor (f.f) varying from 1,11 for sine wave to 1,63 for a single phase unipolar PWM waveform at a modulation index 0,5 and a frequency ratio 12. As the fundamental frequency only 50 Hz was considered, and thus this parameter was not part of the input parameters due to its fixed value.

Table 1 – Network design

Network name	BrSiFF2		
Number of layers	4		
Input layer nodes	4		
Hidden layer-1 nodes	4		
Hidden layer-2 nodes	3		
Output layer nodes	1		
Transfer function	Sigmoid		
Connections	31 (Full)		

The number of cases that are used for training is important. For back propagation neural networks, the more training patterns that are used, the better the resulting model will normally be. For this approach, a total of 450 records were used.

The software permits the use of test sets during training. Test sets are patterns set aside from the training set to test for network overtraining and to check the integrity of the model. The standard deviation between the training output and the set target for the test set used was around 5,5 %, which is a good result considering that different waveforms, as PWM, are considered. Table 2 and Table 3 show the performance of the trained neural network considering some points outside and within the training set, respectively.

Table 2 – Error of the specific total loss recalled from the trained neural network compared with the measured values at 1,6 T (point not used during the training)

Input data for recall						
	d	Si	f.f.	Recall	Measured	Error
В (Т)	(10 ³ kg/m ³)	%		1.1.	answer	Wieasureu
1,6	7,85	0,3	1,00	6,457 8	6,235 3	3,56
1,6	7,85	0,3	1,11	6,984 0	6,649 7	5,03
1,6	7,85	0,3	1,19	7,387 3	7,418 5	0,42
1,6	7,85	0,3	1,31	8,016 9	8,057 9	0,51
1,6	7,85	0,3	1,63	9,709 7	10,105 2	3,91

Table 3 – Error of the specific total loss recalled from the trained neural network compared with the measured values at 1,5 T (point used during the training)

Input data				6		
<u>^</u>	d	Si	Si % f.f.		D !!	Error
В (Т)	(10 ³ kg/m ³)	%		1.1.	Measured	Recall
1,5	7,65	3,0	1,00	2,29	2,34	2,44
1,5	7,65	3,0	1,11	2,38	2,52	5,89
1,5	7,65	3,0	1,19	2,73	2,66	2,32
1,5	7,65	3,0	1,31	2,97	2,88	2,73
1,5	7,65	3,0	1,63	3,69	3,52	4,42
1,5	7,80	1,3	1,00	4,77	4,66	2,23
1,5	7,80	1,3	1,11	4,94	5,00	1,10
1,5	7,60	1,3	1,19	5,43	5,25	3,21
1,5	7,80	1,3	1,31	5,77	5,67	1,70
1,5	7,80	1,3	1,63	6,83	6,93	1,37
1,5	7,85	0,3	1,00	5,40	5,58	3,27
1,5	7,85	0,3	1,11	5,77	6,03	4,57
1,5	7,85	0,3	1,19	6,46	6,39	1,13
1,5	7,85	0,3	1,31	7,03	6,96	0,92
1,5	7,85	0,3	1,63	8,63	8,65	0,24

7.4 Modified superposition formula [20]

If the harmonic order is higher than 9, the phase angle influence on the magnetic loss becomes smaller [4]. The conventional superposition principle, which has been used for the analysis of the magnetic loss, is as follows:

$$P_c(J_1, f_1, J_h, nf_1) = P_c(J_1, f_1) + P_c(J_h, nf_1)$$
(23)

where

 J_1 is magnetic polarization of fundamental frequency;

 J_h is magnetic polarization of higher harmonic frequency $f_h = nf_1$;

 f_1 is the fundamental frequency;

n is an integer.

 $P_c(J_1,f_1)$ and $P_c(J_h,nf_0)$ are the magnetic loss which was measured starting from the normally demagnetized state. This method was applied [2], [21], but the magnetic loss can not be predicted using this superposition principle when the polarization is high or its direction is different from rolling direction [21].

Figure 14 shows $\frac{dJ(t)}{dt}$, H(t) and J(t) when only one period of higher harmonic polarization

is included, and Figure 15 shows it's a.c. hysteresis loops under different positions of the minor loop and for different magnetizing direction. It can be seen that this superposition principle is not applicable in high polarization region and in directions different from the rolling direction from Figure 15. Minor loops which are generated in the zero polarization region and the saturation polarization region are quite different, and also depend on the measurement direction.

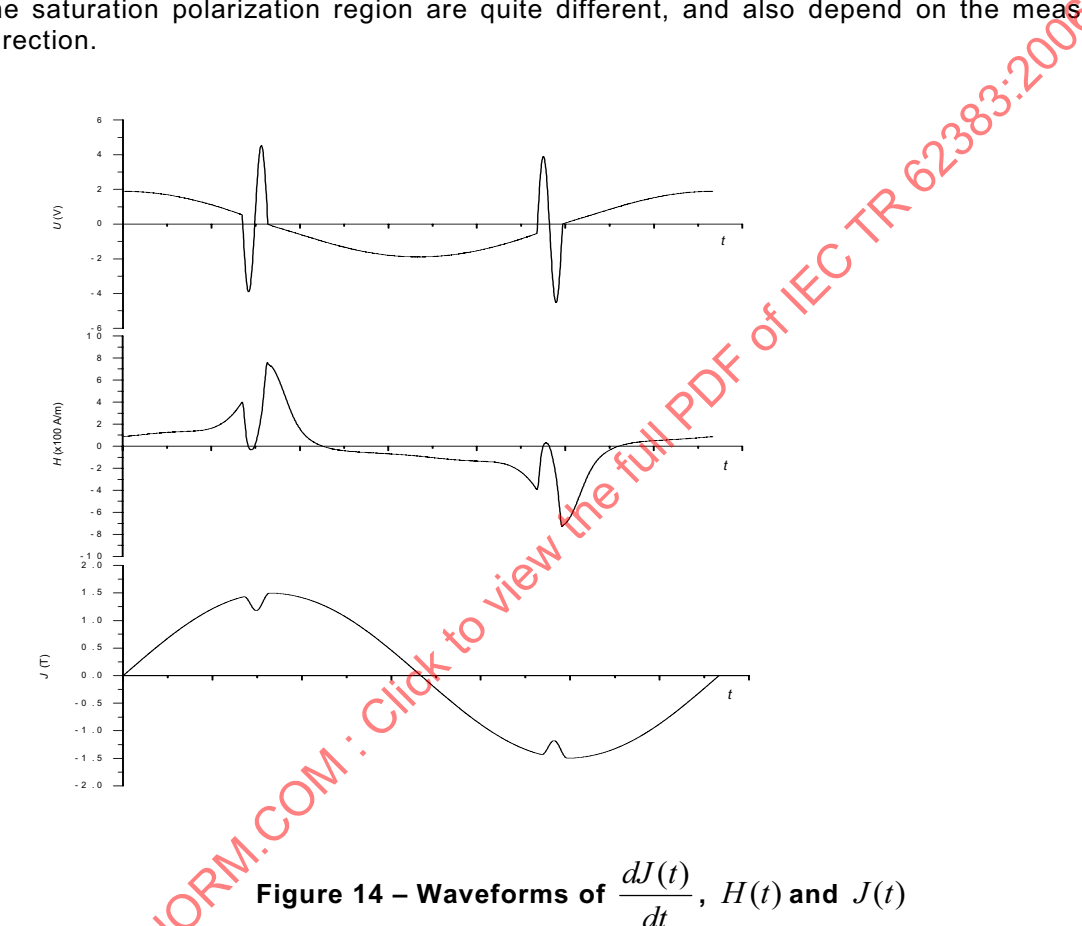


Figure 16 shows that the change of the magnetic loss $P_{\rm c}$ depends on the position of the a.c. minor loop of the higher harmonic relative to the phase of the fundamental wave loop, and on its amplitude. When the higher harmonic amplitude is very small, the magnetic loss $P_{\rm c}$ is not changed with the position of the minor loop. However, when the higher harmonic amplitude was increased, the magnetic loss was increased not only depending on the harmonic amplitude but also depending on the position of the minor loop. When the peak value of the magnetic polarization \hat{J} is 1 T, the magnetic loss $P_{\rm c}$ was not changed depending on the position of the minor loop, but when the peak value of the magnetic polarization \hat{J} is 1,5 T and the harmonic polarization amplitude becomes high, the magnetic loss $P_{\rm c}$ changed strongly depending on the position of minor loop. From this experimental result, it can be concluded that if the minor loop occurs in high polarization regions of the major (fundamental) hysteresis loop, irreversible magnetization rotation, and if it is in the zero polarization region of the major hysteresis loop, irreversible domain wall movement may have an important role in the increasing of the magnetic loss $P_{\rm c}$.

when higher harmonic polarization is included